

Efficient long distance quantum communication

Sreraman Muralidharan^{1*}, Linshu Li^{2*}, Jungsang Kim³, Norbert Lütkenhaus⁴, Mikhail D. Lukin⁵, and Liang Jiang²

¹*Department of Electrical Engineering, Yale University, New Haven, CT 06511 USA*

²*Department of Applied Physics, Yale University, New Haven, CT 06511 USA*

³*Department of Electrical and Computer Engineering, Duke University, Durham, NC 27708 USA*

⁴*Institute of Quantum computing, University of Waterloo, N2L 3G1 Waterloo, Canada and*

⁵*Department of Physics, Harvard University, Cambridge, MA 02138, USA**

(Dated: September 29, 2015)

Despite the tremendous progress of quantum cryptography, efficient quantum communication over long distances ($\geq 1000\text{km}$) remains an outstanding challenge due to fiber attenuation and operation errors accumulated over the entire communication distance. Quantum repeaters (QRs), as a promising approach, can overcome both photon loss and operation errors, and hence significantly speedup the communication rate. Depending on the methods used to correct loss and operation errors, all the proposed QR schemes can be classified into three categories (generations). Here we present the first systematic comparison of three generations of quantum repeaters by evaluating the cost of both temporal and physical resources, and identify the optimized quantum repeater architecture for a given set of experimental parameters. Our work provides a roadmap for the experimental realizations of highly efficient quantum networks over transcontinental distances.

I. INTRODUCTION

First developed in the 1970s, fiber-optic communication systems have boosted the rate of classical information transfer and played a major role in the advent of the information age. The possibility to encode information in quantum states using single photons and transmit them through optical channels has led to the development of quantum key distribution (QKD) systems [1]. However, errors induced by the intrinsic channel attenuation, i.e. loss errors, become a major barrier for efficient quantum communication over continental scales, due to the exponential decay of communication rate [2]. In contrast to classical communication, due to the quantum no-cloning theorem [3], quantum states of photons cannot be amplified without any disturbance. In addition to loss errors, depolarization errors introduced by the imperfect optical channel can impair the quality of the single photon transmitted and hence the quantum information encoded.

To overcome these challenges, quantum repeaters (QRs) have been proposed for the faithful realization of long-distance quantum communication [4]. The essence of QRs is to divide the total distance of communication into shorter intermediate segments connected by QR stations, in which loss errors from fiber attenuation can be corrected. Active mechanisms are also employed at every repeater station to correct operation errors, i.e. imperfections induced by the channel, measurements and gate operations.

As illustrated in Fig. 1, loss errors can be suppressed by either heralded entanglement generation (HEG) [4, 5] or quantum error correction (QEC) [6–10]. During HEG, quantum entanglement can be generated with techniques such as two-photon interference conditioned on the click

patterns of the detectors in between. Loss errors are suppressed by repeating this heralded procedure until the two adjacent stations receive the confirmation of certain successful detection patterns via *two-way* classical signaling.

Alternatively, one may encode the logical qubit into a block of physical qubits that are sent through the lossy channel and use quantum error correction to restore the logical qubit with only *one-way* signaling. Quantum error correcting codes can correct no more than 50% loss rates deterministically due to the no-cloning theorem [9, 11]. To suppress operation errors, one may use either heralded entanglement purification (HEP) [12, 13] or QEC [6–10] as listed in Fig. 1. In HEP, multiple low-fidelity Bell pairs are consumed to probabilistically generate a smaller number of higher-fidelity Bell pairs. Like HEG, to confirm the success of purification, *two-way* classical signaling between repeater stations for exchanging measurement results is required. Alternatively, QEC can correct operation errors using only *one-way* classical signaling, but it needs high fidelity local quantum gates.

Based on the methods adopted to suppress loss and operation errors, we can classify various QRs into three categories as shown schematically in Fig. 2, which we refer to as three generations of QRs [14] [54]. Each generation of QR performs the best for a specific regime of operational parameters such as local gate speed, gate fidelity, and coupling efficiency. In this paper, we consider both the temporal and physical resources consumed by the three generations of QRs and identify the most efficient architecture for different parameter regimes. The results can guide the design of efficient long distance quantum communication links that act as elementary building blocks for future quantum networks.

The paper is organized as follows: In the following section, we will briefly review the characteristics of three generations of QRs. In section III, we use the cost coefficient as an optimization metric to compare the QR per-

*Equal contribution

Errors	Approaches	Examples	Schematics	1G	2G	3G
Loss Error	Heralded Entanglement Generation (HEG)			✓	✓	
	Quantum Error Correction (QEC)					✓
Operation Error	Heralded Entanglement Purification (HEP)			✓		
	Quantum Error Correction (QEC)				✓	✓

Elements:

- Remotely entangled qubit
- Flying qubit (photons)
- CNOT gate
- Qubit in an encoded block
- Measurement (X/Z)
- Teleportation-based Error Correction

FIG. 1: A list of methods to correct loss and operation errors. Depending on the methods used to correct the errors, QRs are categorized into three generations.

formance, and study its dependence on the individual operational parameters including coupling efficiencies, gate fidelities, and gate speed. In section IV, we present a holistic view of the optimization and illustrate the parameter regions where each generation of QRs perform more efficiently than others. In section V, we analyze the advantages and challenges of each generation of QRs and discuss the experimental candidates for their realizations.

II. THREE GENERATIONS OF QUANTUM REPEATERS

The first generation of QRs uses HEG and HEP to suppress loss and operation errors, respectively [4, 5]. This approach starts with purified high-fidelity entangled pairs with separation $L_0 = L_{tot}/2^n$ created and stored in adjacent stations. At k -th nesting level, two entangled pairs of distance $L_{k-1} = 2^{k-1}L_0$ are connected to extend entanglement to distance $L_k = 2^k L_0$ [15]. As practical gate operations and entanglement swapping inevitably cause the fidelity of entangled pairs to drop, HEP can be incorporated at each level of entanglement extension [12, 13]. With n nesting levels of connection and purification, a high-fidelity entangled pair over distance $L_n = L_{tot}$ can

be obtained. The first generation of QRs reduces the exponential overhead in direct state transfer to only polynomial overhead, which is limited by the two-way classical signaling required by HEP between non-adjacent repeater stations. The communication rate still decreases polynomially with distance and thus becomes very slow for long distance quantum communication. The communication rate of the first generation of QRs can be boosted using temporal, spatial, and/or frequency multiplexing associated with the internal degrees of freedom for the quantum memory [5, 16].

The second generation of QRs uses HEG to suppress loss errors and QEC to correct operation errors [6, 7, 17]. First, the encoded states $|0\rangle_L$ and $|+\rangle_L$ are fault-tolerantly prepared using the Calderbank-Shor-Steane (CSS) codes [55] and stored at two adjacent stations. Then, an encoded Bell pair $|\Phi^+\rangle_L = \frac{1}{\sqrt{2}}(|0,0\rangle_L + |1,1\rangle_L)$ between adjacent stations can be created using teleportation-based non-local CNOT gates [18, 19] applied to each physical qubit in the encoded block using the entangled pairs generated through HEG process. Finally, QEC is carried out when entanglement swapping at the encoded level is performed to extend the range of entanglement. The second generation uses QEC to replace HEP and therefore avoids the time-consuming

two-way classical signaling between non-adjacent stations. The communication rate is then limited by the time delay associated with two-way classical signaling between adjacent stations and local gate operations. If the probability of accumulated operation errors over all repeater stations is sufficiently small, we can simply use the second generation of QRs *without* encoding.

The third generation of QRs relies on QEC to correct both loss and operation errors [8–10, 20]. The quantum information can be directly encoded in a block of physical qubits that are sent through the lossy channel. If the loss and operation errors are sufficiently small, the received physical qubits can be used to restore the whole encoding block, which is retransmitted to the next repeater station. The third generation of QRs only needs *one-way* signaling and thus can achieve very high communication rate, just like the classical repeaters only limited by local operation delay. It turns out that quantum parity codes [21] with moderate coding blocks (~ 200 qubits) can efficiently overcome both loss and operation errors [9, 20].

Note that the second and third generations of QRs can achieve communication rate much faster than the first generation over long distances, but they are technologically more demanding. For example, they require high fidelity quantum gates as QEC only works well when operation errors are below the fault tolerance threshold. The repeater spacing for the third generation of QRs is smaller compared to the first two generation of QRs because error correction can only correct a finite amount of loss errors. Moreover, quantum error correcting codes can correct only up to 50% loss error rates deterministically, which restricts the applicable parameter range for the third generation of QRs [9].

III. COMPARISON OF THREE GENERATIONS OF QRs

To present a systematic comparison of different in terms of efficiency, we need to consider both temporal and physical resources. The temporal resource depends on the rate, which is limited by the time delay from the two-way classical signaling (first and second generations) and the local gate operation (second and third generations) [22]. The physical resource depends on the total number of qubits needed for HEP (first and second generations) and QEC (second and third generations) [9, 23]. We propose to quantitatively compare the three generations of QRs using a cost function [9] related to the required number of qubit memories to achieve a given transmission rate. Suppose a total of N_{tot} qubits are needed to generate secure keys at R bits/second, the cost function is defined as

$$C(L_{tot}) = \frac{N_{tot}}{R} = \frac{N_s}{R} \times \frac{L_{tot}}{L_0}, \quad (1)$$

where N_s is the number of qubits needed per repeater station, L_{tot} the total communication distance, and L_0

the spacing between neighboring stations. Since the cost function scales at least linearly with L_{tot} , to demonstrate the additional overhead associated with L_{tot} , the *cost coefficient* can be introduced as

$$C'(L_{tot}) = C/L_{tot}, \quad (2)$$

which can be interpreted as the resource overhead (qubits \times time) for the creation of one secret bit over 1km (with target distance L_{tot}). Besides the fiber attenuation (with $L_{att} = 20$ km), the cost coefficient also depends on other experimental parameters, in particular the coupling efficiency η_c (see supplementary material), the gate error probability ϵ_G , and the gate time t_0 [56]. For third generation QRs, we restrict the search only up to 200 qubits per logical qubit considering the complexity involved in the production of larger codes and for a fair comparison with second generation of QRs. For simplicity, we will assume that t_0 is independent of code size for small encoded blocks for second and third generation QRs. We will now investigate how C' varies with these parameters for three generations of QRs, and identify the optimum generation of QR depending on the technological capability.

A. Coupling efficiency

The coupling efficiency η_c accounts for the emission of photon from the memory qubit, coupling of the photon into the optical fiber and vice versa, and the final detection of photons. The first and second generations of QRs use HEG compatible with arbitrary coupling efficiency, while the third generation relies on QEC requiring the overall transmission (including the coupling efficiency η_c and the channel transmission) to be at least above 50% [9, 24]. As illustrated in Fig. 3, for high coupling efficiency ($\eta_c \gtrsim 90\%$) the third generation of QRs has an obvious advantage over the other generations due to the elimination of two-way classical signaling. As the coupling efficiency is reduced and approaches ($\sim 90\%$) for quantum parity codes, the size of the coding block quickly increases and it becomes less favorable to use this approach since we restrict the size of the encoded block for third generation of QRs. For coupling efficiency below $\sim 90\%$, the optimization chooses the first and second generations of QRs, and then C' is proportional to η_c^{-2} for HEG protocols heralded by two-photon detector click patterns.

If the gate error becomes large (e.g., $\epsilon_G = 10^{-2}$), the capability of correcting loss errors will be compromised for the third generation QRs. Similar trends can be observed as we fix ϵ_G and increase L_{tot} . In contrast to the third generation QRs, the first and second generation QRs with HEG works well even for low coupling efficiencies.

	First Generation QR	Second Generation QR	Third Generation QR
Schematic Architecture			
Loss Error	HEG (two-way signaling)	HEG (two-way signaling)	QEC (one-way signaling)
Operation Error	HEP (two-way signaling)	QEC (one-way signaling)	QEC (one-way signaling)
Procedure	<ol style="list-style-type: none"> 1. Create entangled pairs over L_0 between adjacent stations 2. At k-th level, connect two pairs over L_k and extend to $L_{k+1}=2L_k$, followed by HEP. 3. After n nesting levels, obtain high-fidelity pair over $L_{tot}=2^n \times L_0$ 	<ol style="list-style-type: none"> 1. Prepare encoded states $0\rangle_L$ and $+\rangle_L$ 1. Use teleportation-based non-local CNOT gates to create encoded Bell pairs between adjacent stations. 2. Connect intermediate stations to create long distance encoded Bell pair 	<ol style="list-style-type: none"> 1. Encode information with a block of qubits that are sent through a lossy channel 2. Use QEC to correct both loss and operation errors 3. Relay the encoded information to the next station; and repeat steps 2 & 3.
Inverse Rate ($1/R$)	$\text{Poly}(L_{tot}/c)$	$L_0/c \times \text{PolyLog}(L_{tot})$	$t_0 \times \text{PolyLog}(L_{tot})$
Cost Coefficient (C')	$\text{Poly}(L_{tot})$	$\text{PolyLog}(L_{tot})$	$\text{PolyLog}(L_{tot})$

FIG. 2: Comparison of three generations of QRs.

B. Speed of quantum gates

We investigate the performance of different generations of QRs for different gate times in the range $0.1\mu s \leq t_0 \leq 100\mu s$. As shown in Fig. 4, for high speed quantum gates ($t_0 \lesssim 1\mu s$) the third generation of QRs provides a very fast communication rate, which makes it the most favorable protocol, with $C' \propto t_0$. For slower quantum gates ($t_0 \gtrsim 10\mu s$), the gate time becomes comparable or even larger than the delay of two-way classical signaling between adjacent stations ($t_0 \gtrsim \frac{L_0}{c} \approx \frac{L_{att}}{c}$); as the third generation of QRs loses its advantage in communication rate, the second generation of QRs with less physical resources becomes the optimized QR protocol, with almost constant C' for a wide range of t_0 .

We notice that for small gate error and intermediate distance (e.g., $\epsilon_G = 10^{-4}$ and $L_{tot} = 1000\text{km}$ appeared in Fig. 3a and 4a), encoding might not even be necessary for the second generation of QRs, because the accumulated errors over the entire repeater network are within the tolerable range for quantum communication ($\epsilon_G \frac{L_{tot}}{L_{att}} \lesssim 0.1$). However, for larger error probability or longer distances

($\epsilon_G \frac{L_{tot}}{L_{att}} \gg 0.1$), encoding is required for the second generation QRs[57]. The cost coefficient for the first generation of QRs ($C' > 1 \frac{\text{qubit} \times \text{sec}}{\text{sb}it \times \text{km}}$) lies beyond the scope of Fig. 4, with little dependence on t_0 that is mostly negligible compared to the two-way classical signaling between non-adjacent stations ($\frac{L_{tot}}{c} > 10\text{ms}$).

C. Gate fidelity

The three generations of QRs have different thresholds in terms of gate error probability ϵ_G . The first generation relies on HEP with the highest operation error threshold up to about 3% [4]. The second and third generations both use QEC to correct operation errors, with error correction thresholds of approximately 1% [25]. The gate error threshold of the second generation is slightly lower than that of the third generation, because of the extra gates required for teleportation-based non-local CNOT gates and entanglement swapping in the second generation of QRs (See supplementary material). However, since we restrict the size of the encoded block for third

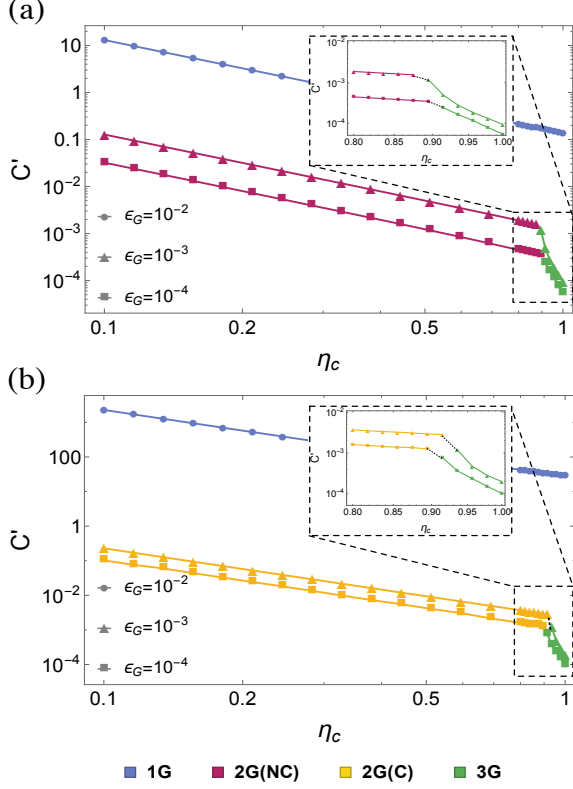


FIG. 3: The optimized cost coefficient \dot{C} as a function of η_c for $t_0 = 1\mu\text{s}$, $\epsilon_G \in \{10^{-2}, 10^{-3}, 10^{-4}\}$, and a) $L_{tot} = 1000\text{km}$, b) $L_{tot} = 10,000\text{km}$. The associated optimized QR protocols are indicated in different colors.

generation of QRs, \dot{C} increases exponentially with ϵ_G slightly below the theoretical threshold of quantum parity codes. As illustrated in Fig. 5, for almost perfect coupling efficiency (e.g. $\eta_c = 100\%$) and fast local operation ($t_0 = 1\mu\text{s}$), the third generation using QEC to correct both fiber attenuation loss and operation errors is the optimized protocol for moderate gate errors. For lower coupling efficiencies (e.g. $\eta_c = 30\%$ and 80%) with too many loss errors for the third generation to tolerate, the first and second generations with HEG yield good performance. As ϵ_G increases, there is a transition at about 0.8% (0.6%) below which the second generation is more favorable for 1000km (10000km).

IV. OPTIMUM GENERATION OF QRs

Based on the above analysis of the cost coefficient that depends on the coupling efficiency η_c , the gate time t_0 , and the gate infidelities ϵ_G , we may summarize the results using the bubble plot and the region plot in the three-dimensional parameter space, as shown in Fig. 6. The bubble color indicates the associated optimized QR protocol, and the bubble diameter is proportional to the

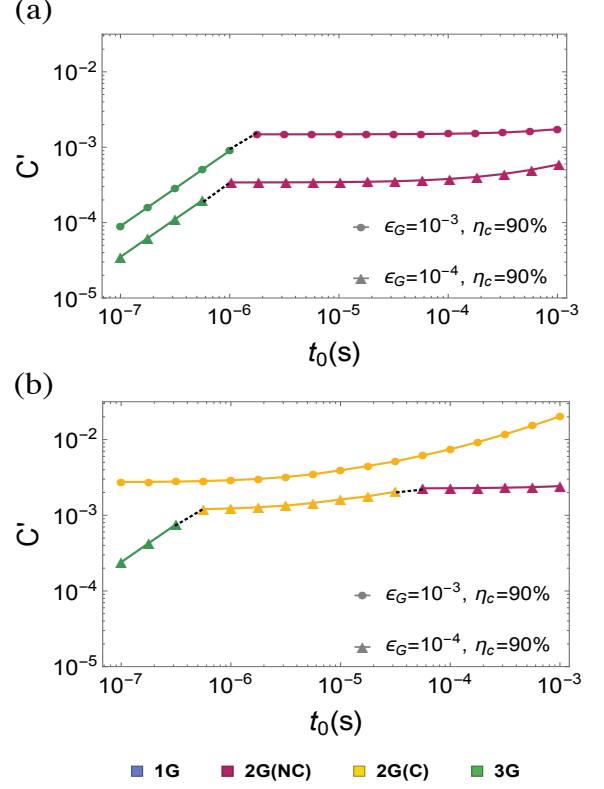


FIG. 4: The optimized cost coefficient \dot{C} as a function of t_0 for $\eta_c = 0.9$, $\epsilon_G \in \{10^{-3}, 10^{-4}\}$, and a) $L_{tot} = 1000\text{km}$, b) $L_{tot} = 10,000\text{km}$. The associated optimized QR protocols are indicated in different colors.

cost coefficient. The parameter space can be divided into the following regions: (I) For high gate error probability ($\epsilon_G \gtrsim 1\%$), the first generation dominates; (II.A) For intermediate gate error probability, but poor coupling efficiency or slow local operation [$0.1 \frac{L_{att}}{L_{tot}} \lesssim \epsilon_G \lesssim 1\%$ and ($\eta_c \lesssim 90\%$ or $t_0 \gtrsim 1\mu\text{s}$)], the second generation *with* encoding is more favorable; (II.B) For low gate error probability, but low coupling efficiency or slow local operation [$\epsilon_G \lesssim 0.1 \frac{L_{att}}{L_{tot}}$ and ($\eta_c \lesssim 90\%$ or $t_0 \gtrsim 1\mu\text{s}$)], the second generation *without* encoding is more favorable; (III) For high coupling efficiency, fast local operation, and low gate error probability ($\eta_c \gtrsim 90\%$, $t_0 \lesssim 1\mu\text{s}$, $\epsilon_G \lesssim 1\%$), the third generation becomes the most favorable scheme in terms of the cost coefficient.

V. DISCUSSIONS

So far, we have mostly focused on the standard procedure of HEG and HEP [4, 5, 12, 13], the CSS-type quantum error correcting codes, and the teleportation-based QEC, which all can be improved and generalized. We have also assumed the simple cost function that scales linearly with the communication time and the total num-

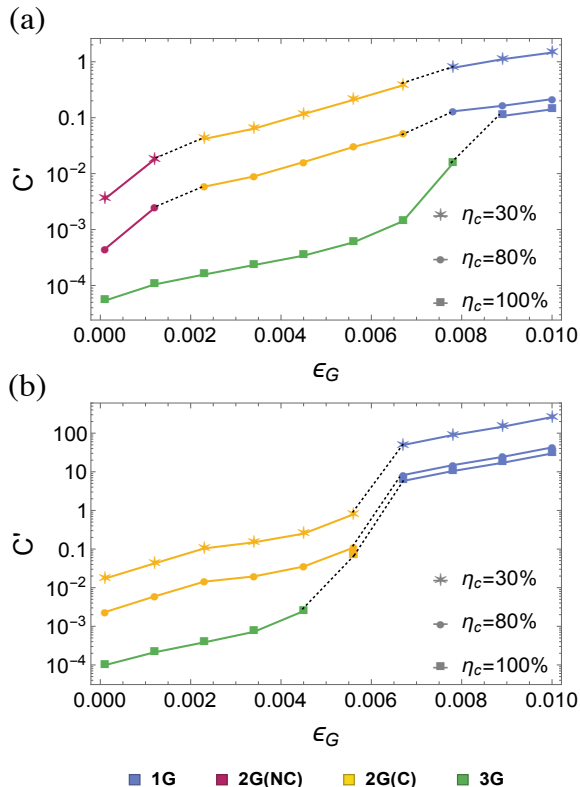


FIG. 5: The optimized cost coefficient C' as a function of ϵ_G for $t_0 = 1\mu s$, $\eta_c \in \{30\%, 80\%, 100\%\}$, and a) $L_{tot} = 1000\text{km}$, b) $L_{tot} = 10,000\text{km}$. The associated optimized QR protocols are indicated in different colors.

ber of qubits. In practice, however, the cost function may have a more complicated dependence on various resources. Nevertheless, we may extend our analysis by using more realistic cost functions to compare various QR protocols. As we bridge the architectural design of QRs and the physical implementations, we may include more variations of HEG, HEP as well as QEC (such as all optical schemes [14, 26]) and use more realistic cost functions, while the general trend and different parameter regions should remain mostly insensitive to these details.

The classification of QR protocols with different performance in the parameter space also provides a guideline for optimized architectural design of QRs based on technological capabilities, which are closely related to physical implementations, including atomic ensembles, trapped ions, NV centers, quantum dots, nanophotonic devices, etc. (1) The atomic ensemble can be used as quantum memory with high coupling efficiency ($> 80\%$ [27, 28]) and compatible with HEG for the first generation of QRs [29]. An important challenge for ensemble-based QRs is the use of non-deterministic quantum gates, which can be partly compensated by *multiplexing* various internal modes of the ensemble memory [5, 16]. Alternatively, the atomic ensemble approach can be sup-

plemented by deterministic atom-photon and atom-atom gates using Rydberg blockade, which can dramatically improve the performance of atomic ensemble approaches and make them compatible with both first and second generations of QRs [30, 31]. (2) The trapped ions, NV centers, and quantum dots all can implement local quantum operations deterministically [32–36], as well as HEG [37–40]. In principle, they are all compatible with the first and second generations of QRs. Although the coupling efficiency is relatively low for single emitters compared to ensembles, it can be boosted with cavity Purcell enhancement [41] (by two orders of magnitude). With high coupling efficiency [42, 43], these systems can also be used for the third generation of QRs. (3) The system of nanophotonic cavity with individual trapped neutral atoms has recently demonstrated quantum optical switch controlled by a single atom with high coupling efficiency [44, 45], which can be used for deterministic local encoding and QEC for the third generation of QRs. Realization of similar techniques with atom-like emitters are likewise being explored. (4) The opto-electromechanical systems have recently demonstrated efficient coherent frequency conversion between optical and microwave photons [46, 47] and can potentially enable using superconducting systems [48] for reliable fast local quantum gates for QRs.

VI. CONCLUSION

In this work, we have classified various QR protocols into three generations based on different methods for suppressing loss and operation errors. Introducing the cost function to characterize both temporal and physical resources, we have systematically compared three generations of QRs for various experimental parameters, including coupling efficiency, gate fidelity, and gate times. There are different parameter regions with drastically different architectural designs of quantum repeaters with different possible physical implementations. Our work will provide a guideline for the optimal design of quantum networks and help in the extension of quantum network of clocks [49], interferometric telescopes [50] and distributed quantum computation [19, 51] to global scales. In the future, the integration of different generations of QRs will enable the creation of a secure quantum internet [52].

Acknowledgements

This work was supported by the DARPA Quiness program, ARL CDQI program, ARO, AFOSR, NBRPC (973 program), the Alfred P. Sloan Foundation and the Packard Foundation. We thank Anna Wang, Hong Tang, Ryo Namiki, Prasanta Panigrahi and Steven Girvin for discussions.

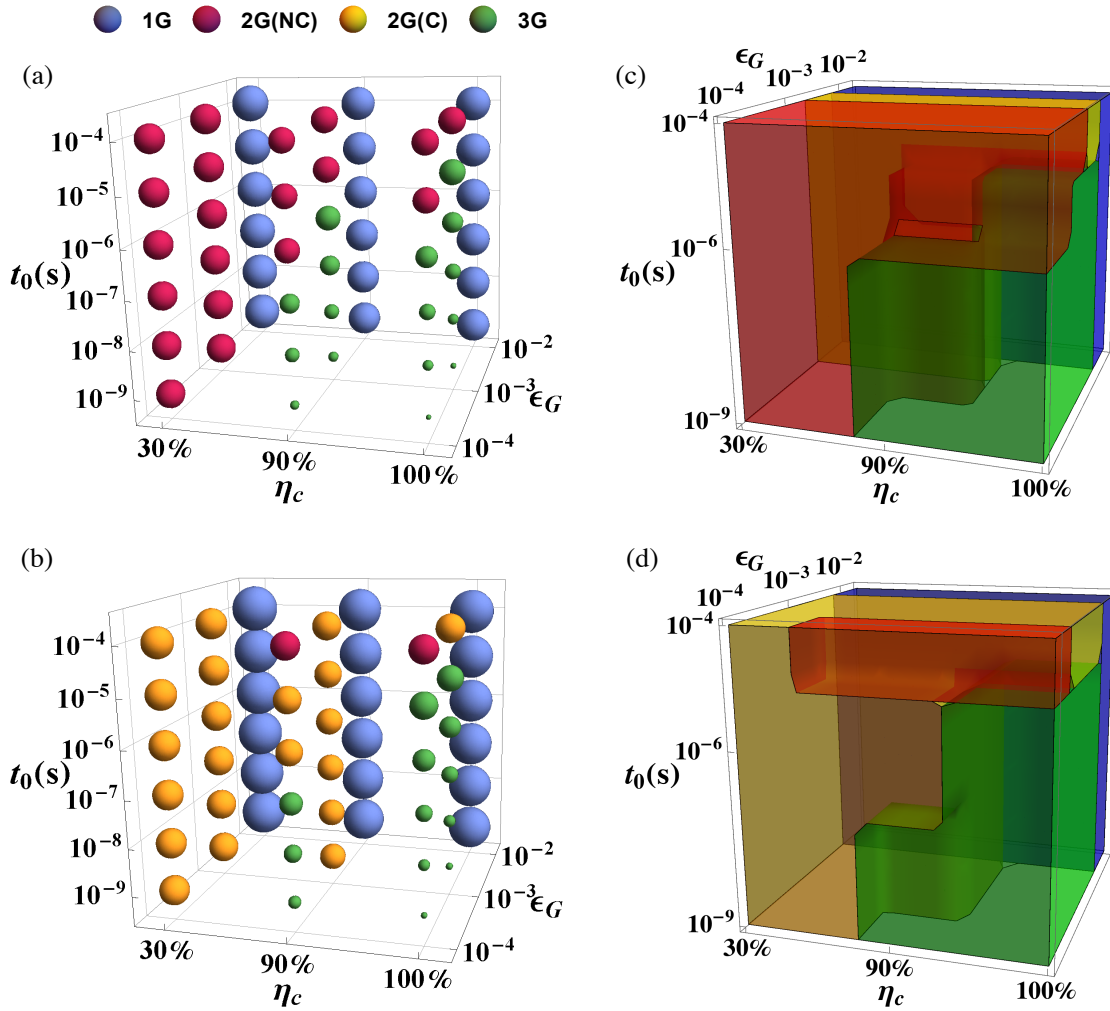


FIG. 6: The bubble plot comparing various QR protocols in the three-dimensional parameter space spanned by η_c , ϵ_G , and t_0 , for a) $L_{tot} = 1000$ km and b) $L_{tot} = 10,000$ km. The bubble color indicates the associated optimized QR protocol, and the bubble diameter is proportional to the cost coefficient. The region plots (c) and (d) showing the distribution of different optimized QR protocol in the three dimensional parameter space for $L_{tot} = 1000$ km and $L_{tot} = 10,000$ km respectively. The region plot (c) contains a yellow region of second generation with encoding, which can be verified in a bubble plot with a finer discretization of ϵ_G .

-
- [1] H.-K. Lo, M. Curty, and K. Tamaki, *Nature Photon.* **8**, 595 (2014).
 [2] M. Takeoka, S. Guha, and M. M. Wilde, *Nature comm.* **5**, 5235 (2014).
 [3] W. K. Wootters and W. H. Zurek, *Nature* **299**, 802 (1982).
 [4] H.-J. Briegel, W. Dür, J. Cirac, and P. Zoller, *Phys. Rev. Lett.* **81**, 5932 (1998).
 [5] N. Sangouard, C. Simon, H. de Riedmatten, and N. Gisin, *Rev. Mod. Phys.* **83**, 33 (2011).
 [6] L. Jiang, J. M. Taylor, K. Nemoto, W. J. Munro, R. Van Meter, and M. D. Lukin, *Phys. Rev. A* **79**, 32325 (2009).
 [7] W. J. Munro, K. A. Harrison, A. M. Stephens, S. J. Devitt, and K. Nemoto, *Nature Photon.* **4**, 792 (2010).
 [8] A. G. Fowler, D. S. Wang, C. D. Hill, T. D. Ladd, R. Van Meter, and L. C. L. Hollenberg, *Phys. Rev. Lett.* **104**, 180503 (2010).
 [9] S. Muralidharan, J. Kim, N. Lütkenhaus, M. D. Lukin, and L. Jiang, *Phys. Rev. Lett.* **112**, 250501 (2014).
 [10] S. Muralidharan, C. L. Zou, L. Li, J. Wen, and L. Jiang, *quant-ph:/1504.08054v1* (2015).
 [11] T. M. Stace, S. D. Barrett, and A. C. Doherty, *Phys. Rev. Lett.* **102**, 200501 (2009).
 [12] D. Deutsch, A. Ekert, R. Jozsa, C. Macchiavello, S. Popescu, and A. Sanpera, *Phys. Rev. Lett.* **77**, 2818 (1996).
 [13] W. Dür, H. J. Briegel, J. I. Cirac, and P. Zoller, *Phys. Rev. A* **59**, 169 (1999).
 [14] W. Munro, K. Azuma, K. Tamaki, and K. Nemoto, *IEEE*

- Jour. Selected topics in Quantum electronics **21**, 1 (2015).
- [15] M. Zukowski, A. Zeilinger, M. A. Horne, and A. K. Ekert, Phys. Rev. Lett. **71**, 4287 (1993).
- [16] M. Bonarota, J. L. L. Gouet, and T. Chaneliere, New J. Phys. **13**, 13013 (2011).
- [17] M. Zwerger, H. J. Briegel, and W. Dür, Scientific reports **4**, 5364 (2014).
- [18] D. Gottesman and I. L. Chuang, Nature **402**, 390 (1999).
- [19] L. Jiang, J. M. Taylor, A. S. Sorensen, and M. D. Lukin, Phys. Rev. A **76**, 62323 (2007).
- [20] W. J. Munro, A. M. Stephens, S. J. Devitt, K. A. Harrison, and K. Nemoto, Nature Photonics **6**, 777 (2012).
- [21] T. C. Ralph, A. J. F. Hayes, and A. Gilchrist, Phys. Rev. Lett. **95**, 100501 (2005).
- [22] L. Jiang, J. M. Taylor, N. Khaneja, and M. D. Lukin, Proc. Natl. Acad. Sci. U. S. A. **104**, 17291 (2007).
- [23] S. Bratzik, H. Kampermann, and D. Bruss, Phys. Rev. A **89**, 32335 (2014).
- [24] C. H. Bennett, D. P. DiVincenzo, and J. A. Smolin, Phys. Rev. Lett. **78**, 3217 (1997).
- [25] E. Knill, Nature **434**, 39 (2005).
- [26] F. Ewert, M. Bergmann, and P. van Loock, quantph:/1503.06777 (2015).
- [27] M. Hosseini, B. M. Sparkes, G. Campbell, P. K. Lam, and B. C. Buchler, Nature Commun. **2**, 174 (2011).
- [28] Y.-H. Chen, M.-J. Lee, I. C. Wang, S. Du, Y.-F. Chen, Y.-C. Chen, and I. A. Yu, Phys. Rev. Lett. **110**, 83601 (2013).
- [29] L. M. Duan, M. D. Lukin, J. I. Cirac, and P. Zoller, Nature **414**, 413 (2001).
- [30] M. D. Lukin, M. Fleischhauer, R. Cote, L. M. Duan, D. Jaksch, J. I. Cirac, and P. Zoller, Phys. Rev. Lett. **87**, 37901 (2001).
- [31] T. Peyronel, O. Firstenberg, Q.-Y. Liang, S. Hofferberth, A. V. Gorshkov, T. Pohl, M. D. Lukin, and V. Vuletic, Nature **488**, 57 (2012).
- [32] J. Chiaverini, D. Leibfried, T. Schaetz, M. D. Barrett, R. B. Blakestad, J. Britton, W. M. Itano, J. D. Jost, E. Knill, C. Langer, R. Ozeri, and D. J. Wineland, Nature **432**, 602 (2004).
- [33] D. Nigg, M. Muller, E. A. Martinez, P. Schindler, M. Hennrich, T. Monz, M. A. Martin-Delgado, and R. Blatt, Science **345**, 302 (2014).
- [34] C. Monroe and J. Kim, Science **339**, 1164 (2013).
- [35] G. Waldherr, Y. Wang, S. Zaiser, M. Jamali, T. Schulthe-Herbruggen, H. Abe, T. Ohshima, J. Isoya, J. F. Du, P. Neumann, and J. Wrachtrup, Nature **506**, 204 (2014).
- [36] J. Medford, J. Beil, J. M. Taylor, E. I. Rashba, H. Lu, A. C. Gossard, and C. M. Marcus, Phys. Rev. Lett. **111**, 50501 (2013).
- [37] H. Bernien, B. Hensen, W. Pfaff, G. Koolstra, M. S. Blok, L. Robledo, T. H. Taminiau, M. Markham, D. J. Twitchen, L. Childress, and R. Hanson, Nature **497**, 86 (2013).
- [38] E. Togan, Y. Chu, A. S. Trifonov, L. Jiang, J. Maze, L. Childress, M. V. G. Dutt, A. S. Sorensen, P. R. Hemmer, A. S. Zibrov, and M. D. Lukin, Nature **466**, 730 (2010).
- [39] H. Bernien, B. Hensen, W. Pfaff, G. Koolstra, M. S. Blok, L. Robledo, T. H. Taminiau, M. Markham, D. J. Twitchen, L. Childress, and R. Hanson, Nature **497**, 86 (2013).
- [40] K. De Greve, L. Yu, P. L. McMahon, J. S. Pelc, C. M. Natarajan, N. Y. Kim, E. Abe, S. Maier, C. Schneider, M. Kamp, S. Hofling, R. H. Hadfield, A. Forchel, M. M. Fejer, and Y. Yamamoto, Nature **491**, 421 (2012).
- [41] T. Kim, P. Maunz, and J. Kim, Phys. Rev. A **84**, 063423 (2011).
- [42] B. Casabone, K. Friebe, B. Brandstätter, K. Schüppert, R. Blatt, and T. E. Northup, Phys. Rev. Lett. **114**, 023602 (2015).
- [43] H. M. Meyer, R. Stockill, M. Steiner, C. Le Gall, C. Matthiesen, E. Clarke, A. Ludwig, J. Reichel, M. Atatüre, and M. Köhl, Phys. Rev. Lett. **114**, 123001 (2015).
- [44] T. G. Tiecke, J. D. Thompson, N. P. de Leon, L. R. Liu, V. Vuletic, and M. D. Lukin, Nature **508**, 241 (2014).
- [45] I. Shomroni, S. Rosenblum, Y. Lovsky, O. Bechler, G. Guendelman, and B. Dayan, Science **345**, 903 (2014).
- [46] T. Bagci, A. Simonsen, S. Schmid, L. G. Villanueva, E. Zeuthen, J. Appel, J. M. Taylor, A. Sorensen, K. Usami, A. Schliesser, and E. S. Polzik, Nature **507**, 81 (2014).
- [47] R. W. Andrews, R. W. Peterson, T. P. Purdy, K. Cicak, R. W. Simmonds, C. A. Regal, and K. W. Lehnert, Nature Phys. **10**, 321 (2014).
- [48] M. H. Devoret and R. J. Schoelkopf, Science **339**, 1169 (2013).
- [49] P. Kómár, E. M. Kessler, M. Bishof, L. Jiang, A. S. Sørensen, J. Ye, and M. D. Lukin, Nature Phys. **10**, 582 (2014).
- [50] D. Gottesman, T. Jennewein, and S. Croke, Phys. Rev. Lett. **109**, 070503 (2012).
- [51] C. Monroe, R. Raussendorf, A. Ruthven, K. R. Brown, P. Maunz, L.-M. Duan, and J. Kim, Phys. Rev. A **89**, 22317 (2014).
- [52] H. J. Kimble, Nature **453**, 1023 (2008).
- [53] M. A. Nielsen and I. Chuang, *Quantum computation and quantum information* (Cambridge University Press, Cambridge, U.K; New York, 2000).
- [54] Note that the combination of QEC for loss errors and HEG for operation errors is sub-optimum compared to the other three combinations.
- [55] CSS codes are considered because of the fault tolerant implementation of preparation, measurement, and encoded CNOT gate [6, 53]
- [56] For simplicity, we assume that the fidelity of physical Bell pairs $F_0 = 1 - \frac{5}{4}\epsilon_g$ achieved with entanglement purification and measurement error probability $\epsilon_m = \frac{\epsilon_g}{4}$ through a verification procedure.
- [57] When ϵ_G increases from 10^{-4} to 10^{-3} , the cost coefficient for the second generation of QR without encoding increases by almost a factor of 10 (Fig. 4a), while the change is less significant for the second and third generations of QRs with encoding (Fig. 4). This is because at the logical level, the change in the effective logical error probability is suppressed for the given set of parameters.

Supplementary Material

Descriptions of error models

a) Two-qubit gate error

Local two-qubit gates, e.g. CNOT gate, are characterized by the gate infidelity ϵ_G . With probability $1 - \epsilon_G$ the desired two-qubit gate is applied, while with probability ϵ_G the state of the two qubits becomes a maximally mixed state. Mathematically the imperfect two-qubit operation on qubit i and j can be expressed as

$$U\rho U^\dagger = (1 - \epsilon_G)U_{ij}\rho U_{ij}^\dagger + \frac{\epsilon_G}{4}\text{Tr}_{ij}[\rho] \otimes I_{ij}, \quad (3)$$

where U_{ij} stands for perfect two-qubit operation on qubit i and j , $\text{Tr}_{ij}[\rho]$ the partial trace over qubit i and j , and I_{ij} the identity operator for qubits i and j .

b) Measurement error

Qubit measurement error is described by the measurement infidelity ξ , which is the probability of a wrong measurement. The error models for projective measurements of states $|0\rangle$ and $|1\rangle$ are

$$\begin{aligned} P_0 &= (1 - \xi)|0\rangle\langle 0| + \xi|1\rangle\langle 1| \\ P_1 &= (1 - \xi)|1\rangle\langle 1| + \xi|0\rangle\langle 0|. \end{aligned} \quad (4)$$

The measurement error can be suppressed by introducing an ancillary qubit for measurement and measuring both the data and the ancillary qubits. If the measurement outcomes don't match, it can be considered as a loss error on that qubit. The contribution of the measurement error to the overall loss error is negligible given the range of the gate error rates ($10^{-4} - 10^{-2}$) we are considering; if they match, then the effective measurement error is given by $\frac{\epsilon_G}{4}$ [8].

c) Memory life-times

In the calculations, the memory qubits are assumed to be perfect, i.e. their life-time is tremendously longer than any characteristic times involved in each scheme. In this sense the most demanding scheme is the first generation, which is optimum at long communication distances, e.g. $L_{tot} = 10^4 km$, and high gate errors. The required coherence time τ for memory qubits is at least limited by the fundamental two-way classical communication time between Alice and Bob

$$t_{c1} = \frac{L_{tot}}{c} \sim 50ms, \quad (5)$$

where $c = 2 \times 10^5 km/s$ is the speed of light in telecom-wavelength optical fiber. Recent experiments with trapped ions, superconducting qubits, solid state spins and neutral atoms have demonstrated quantum memory life-times approaching or exceeding this characteristic value. For the second generation, the characteristic communication time is

$$t_{c2} = \frac{L_{att}}{c} \sim 100\mu s \quad (6)$$

where $L_{att} = 20km$ at telecomm wavelength. The corresponding coherence times are far less demanding than that of the first generation, which relieves the strong life-time requirements on memory qubits and makes the two generations more plausible in practice. Note that when the operation time t_0 becomes comparable or larger than the characteristic communication time, it is then the operation time t_0 that puts limits to the coherence time τ . Third generation QRs are not limited by the two way communication time because it is a fully one way communication scheme.

Quantum entanglement generation, purification and connection

a) Generation of elementary entangled pairs

Heralded entanglement generation with two-photon detection

Using two photon-detection in the middle[1, 2], the success probability of one trial of generating entanglement between two memory qubits in neighboring stations is

$$p = \frac{1}{2}\eta_c^2 e^{-L_0/L_{att}}, \quad (7)$$

where L_0 is the spacing between neighboring stations and η_c is the coupling efficiency accounting for the emission of the photon from the memory qubit, “upload” of the photon into the optical fiber, “download” of the photon from the fiber and the final detection of photons.

Fidelity

Practically an entangled pair generated between neighboring stations may not be a perfect Bell pair and its state is characterized by a density matrix

$$\rho = a|\varphi^+\rangle\langle\varphi^+| + b|\varphi^-\rangle\langle\varphi^-| + c|\psi^+\rangle\langle\psi^+| + d|\psi^-\rangle\langle\psi^-|, \quad (8)$$

where $|\varphi^\pm\rangle = \frac{1}{\sqrt{2}}(|00\rangle \pm |11\rangle)$ and $|\psi^\pm\rangle = \frac{1}{\sqrt{2}}(|01\rangle \pm |10\rangle)$ are the four Bell states. The fidelity of the pair is thus defined as

$$F \equiv a = \langle\varphi^+|\rho|\varphi^+\rangle, \quad (9)$$

Both the first and second generations QRs rely on generating elementary entangled pairs between neighboring repeater stations and then extending the entanglement to longer distances. With the technique of HEP (see the next section), the fidelity of entangled pairs can be boosted to near-unity at the cost of reducing the total number of them and purified pairs can be connected to obtain longer entangled pairs or used as resources for the implementation of remote quantum gates.

However, with imperfect quantum operations and measurements, there is an upper bound on the fidelity of entangled pairs even with entanglement purification. It is in general, a function of the density matrix of raw Bell pairs ρ , gate infidelity ϵ_G and measurement infidelity ξ , and depends on the specific purification protocol one uses. Using Deutsch purification protocol (see the next section), the value of this upper bound can be approximated as

$$\begin{aligned} F_{u.b.} &= 1 - \frac{5}{4}\epsilon_G - \left(\frac{9}{4}\xi + \frac{19}{4}\epsilon_G\right)\epsilon_G + \mathcal{O}(\epsilon_G, \xi)^3 \\ &\approx 1 - \frac{5}{4}\epsilon_G, \end{aligned} \quad (10)$$

in which we assume depolarized states for input raw Bell pairs. This approximate expression holds at small ϵ_G 's ($\lesssim 1\%$). In our calculations and comparison, the temporal resources and physical resources consumed in obtaining purified pairs at the elementary level are not accounted; elementary entangled pairs generated between neighboring stations are assumed to directly take this asymptotic value. The associated additional cost in the purification can be easily added as an overhead into the cost function.

b) Deutsch and Dür purification protocols

In general, despite differences in experimental requirements and efficiencies, the choice of purification protocols will not change the big picture. In this paper, we mainly consider two widely used entanglement purification protocols: Deutsch protocol[3] and Dür[5] protocol. Compared to other purification schemes, the Deutsch protocol reaches higher fidelities with fewer rounds of purification so its upper bound is used as the fidelity of elementary pairs between neighboring stations. The Dür purification protocol is very similar to the Deutsch protocol, except that one of the

two pairs, call auxiliary pair, is never discarded and will be prepared in the same state in each round of purification. This is sometimes also call ‘‘entanglement pumping’’. The Dür purification protocol saves qubit resources by keeping making use of the auxiliary pair, while the state preparation in each purification round is costly in time as a trade-off and if one round fails, the whole purification needs to be started over again.

Here we study the purification with two input pairs characterized by density matrices ρ_1 and ρ_2 ($\rho_1 = \rho_2$ in the case of Deutsch protocol). As mentioned in the previous section, we express the density matrices in the Bell basis $\{|\varphi^+\rangle, |\varphi^-\rangle, |\psi^+\rangle, |\psi^-\rangle\}$. With input states $\{a_1, b_1, c_1, d_1\}$ and $\{a_2, b_2, c_2, d_2\}$, in the presence of gate infidelity ϵ_G and measurement infidelity ξ , the success probability P and the purified state characterized by the diagonal elements $\{a, b, c, d\}$ are the following

$$\begin{aligned}
P &= (1 - \epsilon_G)^2 \{[\xi^2 + (1 - \xi)^2][(a_1 + d_1)(a_2 + d_2) + (b_1 + c_1)(c_2 + b_2)] + 2\xi(1 - \xi)[(a_1 + d_1)(b_2 + c_2) + (b_1 + c_1)(a_2 + d_2)]\} \\
&\quad + \frac{1}{2}[1 - (1 - \epsilon_G)^2] \\
a &= \frac{1}{P} \{(1 - \epsilon_G)^2 [(\xi^2 + (1 - \xi)^2)(a_1 a_2 + d_1 d_2) + 2\xi(1 - \xi)(a_1 c_2 + d_1 b_2)] + \frac{1}{8}[1 - (1 - \epsilon_G)^2]\} \\
b &= \frac{1}{P} \{(1 - \epsilon_G)^2 [(\xi^2 + (1 - \xi)^2)(a_1 d_2 + d_1 a_2) + 2\xi(1 - \xi)(a_1 b_2 + d_1 c_2)] + \frac{1}{8}[1 - (1 - \epsilon_G)^2]\} \\
c &= \frac{1}{P} \{(1 - \epsilon_G)^2 [(\xi^2 + (1 - \xi)^2)(b_1 b_2 + c_1 c_2) + 2\xi(1 - \xi)(b_1 d_2 + c_1 a_2)] + \frac{1}{8}[1 - (1 - \epsilon_G)^2]\} \\
d &= \frac{1}{P} \{(1 - \epsilon_G)^2 [(\xi^2 + (1 - \xi)^2)(b_1 c_2 + c_1 b_2) + 2\xi(1 - \xi)(b_1 a_2 + c_1 d_2)] + \frac{1}{8}[1 - (1 - \epsilon_G)^2]\}
\end{aligned} \tag{11}$$

c) Entanglement Swapping

Entanglement swapping is used in the first generation and second generation without encoding to extend the distance of entanglement. With imperfect CNOT operation and measurements, the diagonal elements $\{a, b, c, d\}$ in the Bell basis of the resulting state obtained from connecting deterministically the input pairs $\{a_1, b_1, c_1, d_1\}$ and $\{a_2, b_2, c_2, d_2\}$ is

$$\begin{aligned}
a &= (1 - \epsilon_G) \{(1 - \xi)^2 (a_1 a_2 + b_1 b_2 + c_1 c_2 + d_1 d_2) + \xi(1 - \xi)[(a_1 + d_1)(b_2 + c_2) + (b_1 + c_1)(a_2 + d_2)] \\
&\quad + \xi^2 (a_1 d_2 + d_1 a_2 + b_1 c_2 + c_1 b_2)\} + \frac{\epsilon_G}{4} \\
b &= (1 - \epsilon_G) \{(1 - \xi)^2 (a_1 b_2 + b_1 a_2 + c_1 d_2 + d_1 c_2) + \xi(1 - \xi)[(a_1 + d_1)(a_2 + d_2) + (b_1 + c_1)(b_2 + c_2)] \\
&\quad + \xi^2 (a_1 c_2 + c_1 a_2 + b_1 d_2 + d_1 b_2)\} + \frac{\epsilon_G}{4} \\
c &= (1 - \epsilon_G) \{(1 - \xi)^2 (a_1 c_2 + c_1 a_2 + b_1 d_2 + d_1 b_2) + \xi(1 - \xi)[(a_1 + d_1)(a_2 + d_2) + (b_1 + c_1)(b_2 + c_2)] \\
&\quad + \xi^2 (a_1 b_2 + b_1 a_2 + c_1 d_2 + d_1 c_2)\} + \frac{\epsilon_G}{4} \\
d &= (1 - \epsilon_G) \{(1 - \xi)^2 (a_1 d_2 + d_1 a_2 + c_1 b_2 + b_1 c_2) + \xi(1 - \xi)[(a_1 + d_1)(b_2 + c_2) + (b_1 + c_1)(a_2 + d_2)] \\
&\quad + \xi^2 (a_1 a_2 + b_1 b_2 + c_1 c_2 + d_1 d_2)\} + \frac{\epsilon_G}{4}
\end{aligned} \tag{12}$$

Note that deterministic entanglement swapping is crucial for long distance quantum communication using QRs. Otherwise the success probability of entangling two qubits separated by L_{tot} drops exponentially as L_{tot} increases.

Implementation and optimization

a) First generation

The first generation of QRs corrects photon loss and operation errors with HEG and HEP, respectively. To overcome the exponential decay in key generation rate induced by photon loss, the total distance L_{tot} is divided into 2^n segments (n is called nesting level [1, 5]) and elementary entangled pairs are generated within each segment, i.e. over repeater spacing $L_0 = \frac{L_{tot}}{2^n}$. An entangled pair covering the total distance L_{tot} can be generated via n levels of entanglement swapping: at each level, two adjacent entangled pairs are connected so that an entangled pair over twice the distance is produced.

However, entanglement swapping necessarily reduces the fidelity of the entangled pairs due to the following two reasons: 1) entanglement swapping involves CNOT operation and measurements, which themselves are imperfect in reality and will introduce noise. 2) Despite imperfect operations, the connection of two imperfect Bell pairs gives a pair with lower fidelity. So multiple rounds of entanglement purification may need to be incorporated at each level to maintain the fidelity, so that the final pair covering L_{tot} is sufficiently robust for secure key distribution.

In the optimization, to determine the best scheme from the first generation QRs, we first fix

- Total distance L_{tot} ,
- Coupling efficiency η_c
- Gate error rate ϵ_G , and thus the fidelity of elementary Bell pairs $F_0 = 1 - \frac{5}{4}\epsilon_G$
- Gate time t_0

and we vary the following parameters:

- Number of nesting level: N
- Number of rounds of purification at each level: $\vec{M} = (M_0, M_1, M_2, \dots, M_N)$
- Choice of entanglement purification protocol: Deutsch or Dür

In carrying out the time resource consumed in generating one remote pair, we adopted similar approximations and derivations as in a previous work[1], with three major changes:

1. We allow arbitrary number of rounds of purification at each level in the optimization, and hence schemes selected could potentially be better optimized.
2. Without losing generality, we use four-state protocol, instead of six-state protocol, in calculating the secure fraction at the asymptotic limit.
3. For long-distance quantum communication, we only consider *deterministic* entanglement swapping and take into account the gate operation time t_0 .

For a given set of N and \vec{M} , detailed derivations of expressions of temporal and physical resource consumed in Deutsch and Dür are given below.

Deutsch et al. entanglement purification protocol

The temporal resource to generate one bit of raw key, T_{Deu} , can be calculated as follows:

$$T_{Deu} = T_0 \cdot \left\{ \left(\frac{3}{2}\right)^N \left(\prod_{x=0}^{N-1} A_{Deu}[N-x] \right) \left(\frac{1}{P_0} A_{Deu}[0] + B_{Deu}[0] \right) + \sum_{y=1}^N \left(\frac{3}{2}\right)^{N-y} B_{Deu}[y] \prod_{x=0}^{N-(y+1)} A_{Deu}[N-x] \right. \\ \left. + \frac{t_0}{T_0} \sum_{y=1}^N \left(\frac{3}{2}\right)^{N-y} \prod_{x=0}^{N-y} A_{Deu}[N-x] \right\}, \quad (13)$$

where

$$A_{Deu}[i] \equiv \left(\frac{3}{2}\right)^{M_i} \prod_{x=0}^{M_i-1} \frac{1}{P_{Deu}(M_i - x, i)} \\ B_{Deu}[i] \equiv \left(\frac{t_0}{T_0} + 2^i\right) \sum_{y=0}^{M_i-1} \left(\frac{3}{2}\right)^y \prod_{x=0}^y \frac{1}{P_{Deu}(M_i - x, i)}. \quad (14)$$

Here, $A_{Deu}[i]$ accounts for the time consumed in the preparation of Bell pairs for purification, and $B_{Deu}[i]$ includes gate operation time and the *two-way* classical signaling time associated with confirming the success of purification. $P_{Deu}(i, j)$ is the success probability of the i^{th} -round of purification at the j^{th} nesting level with Deustch purification

protocol. $T_0 = \frac{L_0}{c}$ is the time unit for the *two-way* classical signaling between neighboring stations, where $c = 2 \times 10^5 \text{ km/s}$ in optical fiber. The secure key generation rate, R_{secure} (sbit/s), can be written as

$$R_{secure}^{Deu} = r_{secure} \cdot \frac{1}{T_{Deu}}, \quad (15)$$

where r_{secure} is the asymptotic secure fraction and in the four-state protocol can be approximately expressed as

$$r_{secure} = \text{Max}[1 - 2h(Q), 0], \quad (16)$$

where $Q = \frac{Q_X + Q_Z}{2}$ is the average quantum bit error rate (QBER) and $h(Q) = -Q \log_2 Q - (1 - Q) \log_2(1 - Q)$ is the binary entropy function. $Q_{X/Z}$ can be calculated from the density matrix of the entangled shared by Alice and Bob in the end. The physical resource, in terms of the number of memory qubits, consumed at half a station can be written as

$$Z_{Deu} = 2^{\sum_{i=0}^{N+1} M_i}, \quad (17)$$

and the cost function becomes

$$C = \frac{2^{N+1} \cdot Z_{Deu}}{R_{secure}^{Deu}}. \quad (18)$$

Dür et al. entanglement purification protocol

The temporal resource to generate one bit of raw key, $T_{Dür}$, can be calculated as follows:

$$\begin{aligned} T_{Dür} = T_0 \cdot \{ & \left(\frac{3}{2}\right)^N \left(\frac{1}{P_0} A_{Dür}[0] + B_{Dür}[0]\right) \left(\prod_{x=0}^{N-1} A_{Dür}[N-x]\right) + \sum_{y=1}^N \left(\frac{3}{2}\right)^{N-y} B_{Dür}[y] \prod_{x=0}^{N-(y+1)} A_{Dür}[N-x] \\ & + \frac{t_0}{T_0} \sum_{y=1}^N \left(\frac{3}{2}\right)^{N-y} \prod_{x=0}^{N-y} A_{Dür}[N-x] \}, \end{aligned} \quad (19)$$

where,

$$\begin{aligned} A_{Dür}[i] &\equiv \prod_{x=0}^{M_i-1} \frac{1}{P_{Dür}(M_i - x, i)} + \sum_{y=0}^{M_i-1} \prod_{x=0}^y \frac{1}{P_{Dür}(M_i - x, i)} \\ B_{Dür}[i] &\equiv \left(\frac{t_0}{T_0} + 2^i\right) \sum_{y=0}^{M_i-1} \prod_{x=0}^y \frac{1}{P_{Dür}(M_i - x, i)}. \end{aligned} \quad (20)$$

Here, $A_{Dür}[i]$ accounts for the time consumed in the preparation of Bell pairs for purification (notice the extra term due to entanglement pumping), and $B_{Dür}[i]$ includes gate operation time and the *two-way* classical signaling time associated with confirming the success of purification. $P_{Dür}(i, j)$ is the success probability of the i^{th} -round of purification at the j^{th} nesting level with Dür purification protocol. Because of the unique entanglement pumping mechanism, the physical resource consumed at half a station is reduced compared to Deustch purification protocol and expressed as

$$Z_{Dür} = N + 2 - |\{M_i : M_i = 0\}|. \quad (21)$$

The derivations of secure key generation rate and hence cost function are similar to those in the previous section.

b) Second generation without encoding

The second generation of QRs relies on generating encoded Bell pairs between neighboring stations and performing error correction during entanglement swapping at the encoded level. With encoding and error correction, physical gate error rates and imperfections in raw Bell pairs are suppressed to higher orders and thus entanglement can be

extended to very long distances with high fidelity. However, if we are interested in the best schemes at low gate error rate $\epsilon \lesssim 10^{-3}$ and total distance $L_{tot} \sim 10^3 km$, the encoding may turn out unnecessary and resources can be saved by simply generating elementary pairs between neighboring stations and implementing entanglement swapping. Fixing the same parameters as the previous section, we vary the following parameters

- Number of memory qubits per half station: N
- Spacing between neighboring stations: L_0
- Number of rounds of elementary entanglement generation trial: $n_{E.G.}$

The secure key generation rate, R_{secure} (sbit/s), can be written as

$$R_{secure} = \frac{[1 - Prob(0, n_{E.G.})]^{\lceil \frac{L_{tot}}{L_0} \rceil} \cdot r_{secure}}{n_{E.G.} \cdot (T_0 + t_0)}, \quad (22)$$

where basic communication time $T_0 = \frac{L_0}{c}$ and r_{secure} follows the same definition above. $Prob(i, n_0) = \binom{M}{n_0} p^{n_0} (1-p)^{M-n_0}$ is the probability to generate i elementary pairs with M qubits in the two half nodes after n_0 rounds of entanglement generation. Therefore, $1 - Prob(0, n_{E.G.})$ means the probability to have *at least* one entangled pair between two neighboring stations. Note that frequency and spatial multiplexing may needed to be incorporated during the transmission of flying qubits and entanglement swapping, respectively. The cost function that will be optimized can be written as

$$C = \frac{2M \cdot \lceil \frac{L_{tot}}{L_0} \rceil}{R_{secure}}. \quad (23)$$

c) Second generation with encoding

For second generation QRs with encoding, encoded Bell pairs are created between neighboring repeater stations and later an encoded entanglement swapping operation is performed at every QR station to generate an encoded Bell pair between distant stations. As in the case of first generation QRs, Bell pairs are generated using HEG between neighboring stations with a high fidelity. These Bell pairs are used as a resource to perform teleportation based CNOT gates between neighboring stations, thereby realizing an encoded CNOT operation between neighboring QR stations. The depolarization error on the data qubits can be modeled as

$$\rho' = \mathcal{E}(\rho) = (1 - \epsilon_d) \rho + \frac{\epsilon_d}{4} \sum_{k=0}^3 \sigma_k \rho \sigma_k. \quad (24)$$

The probability of an error being detected in any one (X or Z) of the measurements is given by,

$$\epsilon_{X/Z} = \epsilon_d + \epsilon_G + 2\xi + \frac{2}{3}(1 - F_0) + O(\epsilon_G, \xi)^2 \quad (25)$$

Any $[[N, k, 2t + 1]]$ CSS code can correct up to t X-errors and t Z-errors respectively. Taking this into account, the probability of correctly and incorrectly decoding the qubit are given by,

$$p_{correct(X/Z)}^{2G} = \sum_{k=0}^t \binom{N}{k} \epsilon_{X/Z}^k (1 - \epsilon_{X/Z})^{(N-k)}, \quad (26)$$

$$p_{incorrect(X/Z)}^{2G} = \sum_{k=t+1}^N \binom{N}{k} \epsilon_{X/Z}^k (1 - \epsilon_{X/Z})^{(N-k)} \quad (27)$$

respectively. Accounting for logical errors in odd number of repeater stations, quantum bit error rates for X and Z basis after R repeater stations is given by,

$$Q_{(X/Z)} = \frac{1}{2} \left[1 - \left(p_{correct(X/Z)}^{2G} - p_{incorrect(X/Z)}^{2G} \right)^R \right]. \quad (28)$$

Where the effective quantum bit error rate is given by $Q = \frac{1}{2} (Q_X + Q_Z)$. The success probability of the protocol is conditioned on having enough Bell pairs between neighboring stations to apply a teleportation based CNOT gate. We can then obtain the key generation rates similar to the case of second generation without encoding. We consider the Steane [[7,1,3]] code, Golay [[23,1,7]] code and the QR [[103,1,19]] codes in our optimization.

d) Third generation QRs

Third generation QRs rely on encoded qubits to relay data from one repeater station to the next where an error correction operation is performed. Since there is just one round of upload and download between the memory qubit and the fiber for third generation QRs, the probability that the photon reaches the neighboring station is given by $\eta_c e^{-L_0/L_{att}}$. Unlike second generation QRs with encoding, teleportation based error correction (TEC) is performed within every repeater station locally for third generation QRs. Teleportation based error correction requires an encoded CNOT gate between the incoming encoded qubit block (with loss and operation errors) and encoded qubit block (with no loss errors) at every repeater station. R is the incoming encoded block and S is the encoded block from the encoded Bell pair. The depolarization errors on blocks R and S can be modeled as,

$$\rho'_R = \mathcal{E}_R(\rho_{RS}) = \eta(1 - \epsilon_d) \rho_R + \frac{\eta \epsilon_d}{4} \sum_{k=0}^3 \sigma_k \rho \sigma_k + (1 - \eta) |vac\rangle\langle vac| \quad (29)$$

$$\rho'_S = \mathcal{E}_S(\rho_{RS}) = (1 - \epsilon_d) \rho_S + \frac{\epsilon_d}{4} \sum_{k=0}^3 \sigma_k \rho \sigma_k, \quad (30)$$

To be consistent with [7], we make the following assumptions in our analysis. 1) Errors are not propagated between repeater stations. 2) Each qubit has an independent error. The effective X/Z error detected at the measurement (Y errors are detected in both X and Z measurements) is given by,

$$\epsilon_{X/Z} = \left(\epsilon_d + \frac{\epsilon_G}{2} + \xi \right) \eta + O(\epsilon_G, \xi)^2. \quad (31)$$

We consider (n,m) quantum parity codes given by

$$|\pm\rangle_L = \frac{1}{2^{n/2}} (|0\rangle^{\otimes m} \pm |1\rangle^{\otimes m})^{\otimes n}, \quad (32)$$

in our analyses. The outcome of the measurement of the logical operators X_L and Z_L for TEC can be determined through a majority voting procedure discussed in detail in [7]. There are three possible outcomes of the majority voting procedure: a) Heralded failure leading to the inability to perform a majority voting with probability $p_{unknown(X/Z)}^{3G}$. b) Perform a majority voting and correctly decoding the qubit with probability $p_{correct(X/Z)}^{3G}$. c) Perform a majority voting and incorrectly decoding the qubit with probability $p_{incorrect(X/Z)}^{3G}$. Here, we treat the three events as independent for the measurement of the logical operators for simplicity. The success probability accounting for no heralded failure in any one of the R repeater stations is given by,

$$P_{succ} = (1 - p_{unknown(X/Z)}^{3G})^R \quad (33)$$

Accounting for errors in odd number of repeater stations, the quantum bit error rate for X/Z bases is given by,

$$Q_{(X/Z)} = \frac{1}{2} \left[1 - \left(\frac{p_{correct(X/Z)}^{3G} - p_{incorrect(X/Z)}^{3G}}{p_{correct(X/Z)}^{3G} + p_{incorrect(X/Z)}^{3G}} \right)^R \right] \quad (34)$$

The asymptotic secure key generation rates is given by,

$$R_{secure} = \text{Max}\left[\frac{P_{succ}}{t_0}\{1 - 2h(Q)\}, 0\right], \quad (35)$$

where t_0 is the time taken to apply local operations. The cost function for the (n, m) quantum parity codes is given by

$$C = \frac{2m \cdot n \lceil \frac{L_{tot}}{L_0} \rceil}{R_{secure}}. \quad (36)$$

For a fair comparison with second generation QRs, where a largest code of $[[103, 1, 19]]$ code was used, we restrict the maximum qubits for the third generation quantum repeaters to be 200. We restrict the search of (n, m) quantum parity codes within the range $2 \leq (m, n) \leq 20$.

-
- [1] Sangouard, N., Dubessy, R. & Simon, C. Quantum repeaters based on single trapped ions. *Phys. Rev. A* **79**, 042340 (2009)
 - [2] Sangouard, N., Simon, C., de Riedmatten, H. & Gisin, N. Quantum repeaters based on atomic ensembles and linear optics. *Rev. Mod. Phys.* **83**, 33–80 (2011).
 - [3] Deutsch, D. *et al.* Quantum privacy amplification and the security of quantum cryptography over noisy channels. *Phys. Rev. Lett.* **77**, 2818 (1996)
 - [4] Briegel, H-J., Dür, W., Cirac, J. I. & Zoller, P. Quantum Repeaters: The Role of Imperfect Local Operations in Quantum Communication. *Phys. Rev. Lett.* **81**, 5932 (1998).
 - [5] Dür, W., Briegel, H-J., Cirac, J. I. & Zoller, P. Quantum repeaters based on entanglement purification. *Phys. Rev. A* **59**, 169 (1999).
 - [6] Bratzik, S., Abruzzo, S., Kampermann, H. & Bru, D. Quantum repeaters and quantum key distribution: The impact of entanglement distillation on the secret key rate. *Phys. Rev. A* **87**, 062335 (2013)
 - [7] Muralidharan, S., Kim, J., Lütkenhaus, N., Lukin, M. & Jiang, L. Ultrafast and Fault-Tolerant Quantum Communication across Long Distances. *Phys. Rev. Lett.* **112**, 250501 (2014)
 - [8] Knill, E. Quantum computing with realistically noisy devices. *Nature(London)* **434**, 39-44 (2005)